

Population properties of neutron stars in the coalescing compact binaries

YIN-JIE LI (李银杰) ^{1,2} SHAO-PENG TANG (唐少鹏) ^{1,2} YUAN-ZHU WANG (王远瞩) ¹
QIANG YUAN (袁强) ^{1,2} YI-ZHONG FAN (范一中) ^{1,2} AND DA-MING WEI (韦大明) ^{1,2}

¹*Key Laboratory of Dark Matter and Space Astronomy, Purple Mountain Observatory, Chinese Academy of Sciences, Nanjing 210023, People's Republic of China*

²*School of Astronomy and Space Science, University of Science and Technology of China, Hefei, Anhui 230026, People's Republic of China*

(Received ...; Revised ...; Accepted ...)

ABSTRACT

We perform a hierarchical Bayesian inference to investigate the population properties of the coalescing compact binaries involving at least one neutron star (NS). With the current observation data, we can not rule out either of the Double Gaussian, Single Gaussian and Uniform NS mass distribution models, although the mass distribution of the Galactic NSs is slightly preferred by the gravitational wave (GW) observations. The mass distribution of black holes (BHs) in the neutron star-black hole (NSBH) population is found to be similar to that for the Galactic X-ray binaries. Additionally, the ratio of the merger rate densities between NSBHs and BNSs is estimated to be $\sim 3 : 7$. The spin properties of the binaries, though constrained relatively poor, play nontrivial role in reconstructing the mass distribution of NSs and BHs. We find that a perfectly aligned spin distribution can be ruled out, while a purely isotropic distribution of spin orientation is still allowed.

Keywords: Gravitational waves—Neutron stars—Binaries: close

1. INTRODUCTION

Recently, the observations of gravitational wave (GW) signals from two neutron star-black hole (NSBH) coalescences, i.e., GW200105 and GW200115, have been reported by LIGO/Virgo/KAGRA Collaboration (LVK; Abbott et al. 2021a). These two events are also the first confident observations of NSBH binaries in the Universe, although previously the modeling of the kilonova emission of hybrid GRB 060614 was also strongly in favor of a NSBH merger origin (Yang et al. 2015; Jin et al. 2015). Since the first successful detection of GW (Abbott et al. 2016) in 2015, about ~ 50 compact binary coalescences (CBCs) have been formally reported (Abbott et al. 2021b), including several mergers involving at least one neutron star and some events from binary black hole (BBH) coalescences (e.g., Abbott et al. 2017, 2020a,b,c). With a rapidly increasing sample of GW events, our understanding of the population properties of the stellar BHs in the Universe has been advanced (e.g., Abbott et al. 2021c; Wang et al. 2021; Li et al. 2021), and some formation/evolution processes of the compact binaries are being revealed (e.g., Safarzadeh & Wysocki 2021; Tang et al. 2021). However, due to the limited observation of NSBH and BNS mergers up to now, the population properties of these kinds of coalescence systems are hard to probe. Moreover, Tang et al. (2020) found that the misclassification of BBH into NSBH makes it more challenging to reconstruct the mass function of the BHs. Thanks to the observation of Galactic radio pulsars, a large number of NS masses have been measured (Özel & Freire 2016; Shao et al. 2020). The mass distribution of these Galactic NSs has been investigated and a double-Gaussian model with two peaks at $\sim 1.35M_{\odot}$ and $\sim 1.9M_{\odot}$ are found to be able to well reproduce the data (Alsing et al. 2018; Shao et al. 2020). Nevertheless, it is very interesting to investigate the mass distribution of NSs in the Universe, and the GW observations provide the unprecedented valuable chance. Recently, Landry & Read (2021) tried to reconstruct the mass distribution of this extragalactic population of NSs and found out that the mass function seems to be more

consistent with a uniform distribution than the bimodal Galactic population. However, in their hierarchical inferences, just the masses of compact objects have been taken into account, and the spin information of the compact binaries has not been included. As found in the literature, for the GW events involving at least one BH, there is mass-spin degeneracy (Pratten et al. 2020). The measurements of both the component masses and misaligned spins are of prime importance in understanding the origin and evolution of astrophysical compact binaries (Rodriguez et al. 2016; Qin et al. 2019, 2018). Binaries born in isolated evolution are expected to form with nearly aligned spins (Kalogera 2000). After considering the supernova kicks, the compact object binaries tend to still have small misalignments (Rodriguez et al. 2016). On the contrary, binaries originated from dynamical capture are expected to have isotropic distribution for their spin orientations (Vitale et al. 2017). By surveying the spin properties of BBH population, Abbott et al. (2021c) find that the current BBH merger events likely originate from both formation channels.

In this work, we perform a hierarchical Bayesian inference to investigate the population properties of NSs that detected by LIGO and Virgo with the information of their masses and spins. In Sec. 2, we introduce the data and the model used for inference, in Sec. 3 we present our modeling results, and Sec. 4 is our conclusion and discussion.

2. METHOD

2.1. Selected events

Our hierarchical analysis is based on the GW events involving at least one NS, which consist of four published confident events, including GW170817, GW190425, GW200105 and GW200115 (Abbott et al. 2017, 2020a, 2021a), and one marginal event, GW190426_152155. Though the nature of GW190425 and GW190426_152155 are not fully solved yet (Han et al. 2020; Li et al. 2020), the former is more likely a BNS and the latter a NSBH (Abbott et al. 2020a, 2021b). Therefore, our data sample includes two BNS events and three NSBH events (or candidate). The parameter estimation results for individual candidate event are from Abbott et al. (2019, 2021b). Since we need the spin information (including spin magnitude and orientation) for each compact object, all the posterior samples should be estimated by the precession waveforms. So in this work we adopt the “IMRPhenomPv2NRT_lowSpin_posterior”, “PhenomPNRT-LS”, “C01:PhenomXPHM_low_spin”, “C01:PhenomXPHM_low_spin”, and “PrecessingSpinIMRHM” posterior samples for GW170817, GW190425, GW200105, GW200115, and GW190426_152155, respectively.

2.2. Models

For the hierarchical population inference, here we consider three typical models for NS mass distribution and two for BH mass distribution. The first NS mass function model is the Double Gaussian scenario,

$$\pi(m_{\text{NS}}|m_{\text{min}}, m_{\text{max}}, \mu_1, \sigma_1, \mu_2, \sigma_2, r_1) = r_1 \mathcal{N}_1(m_{\text{NS}}|\mu_1, \sigma_1)/\Phi_1 + (1 - r_1) \mathcal{N}_2(m_{\text{NS}}|\mu_2, \sigma_2)/\Phi_2, \text{ for } m_{\text{NS}} \in (m_{\text{min}}, m_{\text{max}}). \quad (1)$$

The second is the Single Gaussian model,

$$\pi(m_{\text{NS}}|m_{\text{min}}, m_{\text{max}}, \mu, \sigma) = \mathcal{N}(m_{\text{NS}}|\mu, \sigma)/\Phi, \text{ for } m_{\text{NS}} \in (m_{\text{min}}, m_{\text{max}}). \quad (2)$$

And the third is the Uniform scenario,

$$\pi(m_{\text{NS}}|m_{\text{min}}, m_{\text{max}}) = 1/(m_{\text{max}} - m_{\text{min}}), \text{ for } m_{\text{NS}} \in (m_{\text{min}}, m_{\text{max}}). \quad (3)$$

Motivated by Özel et al. (2010) and Abbott et al. (2021c), we introduce a Truncated Gaussian and a Truncated Power Law for the mass distribution of BHs,

$$\pi(m_{\text{BH}}|m_{\text{low}}, m_{\text{up}}, \mu, \sigma) = \mathcal{N}(m_{\text{BH}}|\mu, \sigma)/\Phi', \text{ for } m_{\text{BH}} \in (m_{\text{low}}, m_{\text{up}}). \quad (4)$$

$$\pi(m_{\text{BH}}|m_{\text{low}}, m_{\text{up}}, \alpha) = \frac{m_{\text{BH}}^{-\alpha}}{\int_{m_{\text{low}}}^{m_{\text{up}}} m^{-\alpha} dm}, \text{ for } m_{\text{BH}} \in (m_{\text{low}}, m_{\text{up}}). \quad (5)$$

In the above equations, m_{NS} and m_{BH} are the mass of NS and BH, while Φ_1 , Φ_2 , Φ , and Φ' are the normalization constants, and other parameters with the priors are described in Table 1.

The parameterization for the component (BH or NS) spin magnitudes and tilts is similar to the DEFAULT model in Abbott et al. (2021c). The spin tilt of each component in a binary is assumed to be independently drawn from the

same underlying distribution, see Eq.(6) below. For simplicity, we use two truncated gaussian to fit the dimensionless spin magnitudes of BHs and NSs (i.e., a_{BH} and a_{NS}), respectively. Therefore, the model of spin reads

$$\pi(z|\zeta, \sigma_t) = \zeta \mathcal{N}(z|1, \sigma_t) / \Phi_z + (1 - \zeta) / 2, \text{ for } z \in (-1, 1), \quad (6)$$

$$\pi(a_{\text{BH}}|\mu_a^{\text{BH}}, \sigma_a^{\text{BH}}) = \mathcal{N}(a_{\text{BH}}|\mu_a^{\text{BH}}, \sigma_a^{\text{BH}}) / \Phi_a^{\text{BH}}, \text{ for } a_{\text{BH}} \in (0, 1), \quad (7)$$

$$\pi(a_{\text{NS}}|\mu_a^{\text{NS}}, \sigma_a^{\text{NS}}) = \mathcal{N}(a_{\text{NS}}|\mu_a^{\text{NS}}, \sigma_a^{\text{NS}}) / \Phi_a^{\text{NS}}, \text{ for } a_{\text{NS}} \in (0, a_{\text{max}}^{\text{NS}}), \quad (8)$$

where $z = \cos \theta_{1,2}$, and $\theta_{1,2}$ is tilt angle between component spin and a binary's orbital angular momentum, Φ_a^{BH} and Φ_a^{NS} are the normalization constants. Since the highest dimensionless NS spin implied by pulsar-timing observations of binaries that merge within a Hubble time is 0.04 (Stovall et al. 2018; Zhu et al. 2018), it's reasonable to set $a_{\text{max}}^{\text{NS}} = 0.05$. All the description of the parameters and the priors of each model are presented in Table 1

Combining the mass and spin models, we get the synthesis models for NSs and BHs,

$$\pi(m_{\text{NS}}, a_{\text{NS}}, z|\mathbf{\Lambda}_{\text{NS}}) = \pi(m_{\text{NS}}|\mathbf{\Lambda}_{\text{NS}}^{\text{m}}) \pi(a_{\text{NS}}|\mathbf{\Lambda}_{\text{NS}}^{\text{a}}) \pi(z|\mathbf{\Lambda}_{\text{z}}), \quad (9)$$

$$\pi(m_{\text{BH}}, a_{\text{BH}}, z|\mathbf{\Lambda}_{\text{BH}}) = \pi(m_{\text{BH}}|\mathbf{\Lambda}_{\text{BH}}^{\text{m}}) \pi(a_{\text{BH}}|\mathbf{\Lambda}_{\text{BH}}^{\text{a}}) \pi(z|\mathbf{\Lambda}_{\text{z}}), \quad (10)$$

where $\mathbf{\Lambda}_{\text{NS}}^{\text{m}}$ ($\mathbf{\Lambda}_{\text{BH}}^{\text{m}}$), $\mathbf{\Lambda}_{\text{NS}}^{\text{a}}$ ($\mathbf{\Lambda}_{\text{BH}}^{\text{a}}$), and $\mathbf{\Lambda}_{\text{z}}$ are the population parameters for mass distribution of NS (BH), spin magnitude of NS (BH), and spin orientations, respectively. And $\mathbf{\Lambda}_{\text{NS}} = \mathbf{\Lambda}_{\text{NS}}^{\text{m}} \cup \mathbf{\Lambda}_{\text{NS}}^{\text{a}} \cup \mathbf{\Lambda}_{\text{z}}$, $\mathbf{\Lambda}_{\text{BH}} = \mathbf{\Lambda}_{\text{BH}}^{\text{m}} \cup \mathbf{\Lambda}_{\text{BH}}^{\text{a}} \cup \mathbf{\Lambda}_{\text{z}}$. Since the secondary objects of all the binaries are NSs, the model for them is

$$\pi(m_2, a_2, z_2|\mathbf{\Lambda}_2) = \pi(m_{\text{NS}}, a_{\text{NS}}, z_2|\mathbf{\Lambda}_{\text{NS}}). \quad (11)$$

While the primary objects can be NSs and BHs, we define r_{BNS} as the fraction of BNS populations, then the model for primary objects becomes

$$\pi(m_1, a_1, z_1|\mathbf{\Lambda}_1) = r_{\text{BNS}} \pi(m_{\text{NS}}, a_{\text{NS}}, z_1|\mathbf{\Lambda}_{\text{NS}}) + (1 - r_{\text{BNS}}) \pi(m_{\text{BH}}, a_{\text{BH}}, z_1|\mathbf{\Lambda}_{\text{BH}}). \quad (12)$$

So the synthesis models for the NSBH and BNS binaries are represented as

$$\pi(\theta|\mathbf{\Lambda}) = \pi(m_2, a_2, z_2, m_1, a_1, z_1|\mathbf{\Lambda}) = \pi(m_2, a_2, z_2|\mathbf{\Lambda}_2) \pi(m_1, a_1, z_1|\mathbf{\Lambda}_1), \quad (13)$$

where θ is event parameters, while $\mathbf{\Lambda}$ is the population parameters for synthesis models, and $\mathbf{\Lambda} = \mathbf{\Lambda}_1 \cup \mathbf{\Lambda}_2 = \mathbf{\Lambda}_{\text{NS}} \cup \mathbf{\Lambda}_{\text{BH}} \cup \{r_{\text{BNS}}\}$. Additionally, in order to test whether the distribution of NSs observed via GW is consistent with that observed electromagnetically in the Galaxy, we fix the parameters of Double Gaussian for NSs as $m_{\text{min}} = 1M_{\odot}$, $m_{\text{max}} = 2.25M_{\odot}$, $\mu_1 = 1.36M_{\odot}$, $\sigma_1 = 0.09M_{\odot}$, $\mu_2 = 1.9M_{\odot}$, $\sigma_2 = 0.5M_{\odot}$, and $r_1 = 0.65$ (Shao et al. 2020). Thus, there are 4 NS mass distribution models (i.e., Double Gaussian, Single Gaussian, Uniform, and Galactic distribution) \times 2 BH mass distribution models (i.e., Truncated Power Law and Truncated Gaussian) \times 1 spin model. In other words we have 8 synthesis models.

2.3. Hierarchical likelihood

With the data of the observed events $\{d\}$ that described in Sec. 2.1, and the population models described in Sec. 2.2, we perform a hierarchical Bayesian inference following Abbott et al. (2021c) and Thrane & Talbot (2019). For the given data $\{d\}$ from N_{det} GW detections, the likelihood of $\mathbf{\Lambda}$ can be expressed as

$$\mathcal{L}(\{d\}|\mathbf{\Lambda}) \propto \prod_{i=1}^{N_{\text{det}}} \frac{\int \mathcal{L}(d_i|\theta_i) \pi(\theta_i|\mathbf{\Lambda}) d\theta_i}{\xi_i(\mathbf{\Lambda})}, \quad (14)$$

where $\xi_i(\mathbf{\Lambda})$ means the detection fraction, and the single-event likelihood $\mathcal{L}(d_i|\theta_i)$ can be estimated using the posterior samples described in Sec. 2.1 (see Abbott et al. (2021c) for detail), then the Eq.(14) takes the form of

$$\mathcal{L}(\{d\}|\mathbf{\Lambda}) \propto \prod_{i=1}^{N_{\text{det}}} \frac{1}{\xi_i(\mathbf{\Lambda})} \frac{1}{n_i} \sum_k^{n_i} \frac{\pi(\theta_i^k|\mathbf{\Lambda})}{\pi_{\phi}(\theta_i^k)}, \quad (15)$$

Table 1. Distribution of the priors for hierarchical Bayesian inference.

Description	Parameters	NS mass distribution priors		
		Double Gaussian	Single Gaussian	Uniform
minimum mass of NSs	$m_{\min}[M_{\odot}]$	U(1,1.3)	U(1,1.3)	U(1,1.3)
maximum mass of NSs	$m_{\max}[M_{\odot}]$	U(1.7,2.9)	U(1.7,2.9)	U(1.7,2.9)
mean of first Gaussian	$\mu_1[M_{\odot}]$	U(1, 2.2)	-	-
mean of second Gaussian	$\mu_2[M_{\odot}]$	U(1, 2.2)	-	-
standard deviation of first Gaussian	$\sigma_1[M_{\odot}]$	U(0.01, 1)	-	-
standard deviation of second Gaussian	$\sigma_2[M_{\odot}]$	U(0.01, 1)	-	-
fraction of first Gaussian	r_1	U(0, 1)	-	-
mean of single Gaussian	$\mu[M_{\odot}]$	-	U(1, 2.2)	-
standard deviation of single Gaussian	$\sigma[M_{\odot}]$	-	U(0.01, 1)	-
fraction of BNS population	r_{BNS}	U(0, 1)	U(0, 1)	U(0, 1)
Constraint	-	$m_{\min} < \mu_1 < \mu_2 < m_{\max}$	$m_{\min} < \mu < m_{\max}$	-
		BH mass distribution priors		
		Truncated Power Law		Truncated Gaussian
low boundary of BH mass distribution	$m_{\text{low}}[M_{\odot}]$	U(3,8)		U(3,8)
high boundary of BH mass distribution	$m_{\text{up}}[M_{\odot}]$	U(10,30)		U(10,30)
negative spectral index of Power law	α	U(-4, 12)		-
mean of Gaussian for BH	$\mu_{\text{BH}}[M_{\odot}]$	-		U(5, 15)
standard deviation of Gaussian for BH	$\sigma_{\text{BH}}[M_{\odot}]$	-		U(0.5, 10)
Constraint	-	-		$m_{\text{low}} < \mu_{\text{BH}} < m_{\text{up}}$
		spin priors		
mean of spin for NS	$\mu_{\text{a}}^{\text{NS}}$		U(0, 0.05)	
standard deviation of spin for NS	$\sigma_{\text{a}}^{\text{NS}}$		U(0.01, 0.05)	
mean of spin for BH	$\mu_{\text{a}}^{\text{BH}}$		U(0, 0.99)	
standard deviation of spin for BH	$\sigma_{\text{a}}^{\text{BH}}$		U(0.01, 0.25)	
width of spin misalignment for field mergers	σ_{t}		U(0.01, 4.)	
fraction of field mergers	ζ		U(0, 1)	

Note. Here ‘U’ means the uniform distribution.

where $\pi_{\phi}(\theta_i^k)$ is the default prior used for initial parameter estimation, and n_i is the size of posterior samples. For the estimation of $\xi_i(\mathbf{\Lambda})$, we use a Monte Carlo integral over detected injections as introduced in Abbott et al. (2021c) and Tiwari (2018). And the injection campaigns are made by injecting simulated signal to the LIGO-Virgo detectors with noise curves¹. We define the threshold of the injected signal being detected as the network signal-to-noise ratio greater than 12. For the hierarchical Bayesian inference, we use the Bilby package (Ashton et al. 2019) and Dynesty sampler (Speagle 2020).

3. RESULTS

In this section we report the results obtained by the synthesis hierarchical models described in Sec. 2. With the logarithm Bayes factors of all models summarized in Table 2, we can conclude that all three NS mass function models are comparable. Nevertheless, it is interesting to see that the Galactic model (i.e., the fixed Double Gaussian model) is slightly preferred than the others. As for BH mass distribution, we find that the Truncated Power Law model has a preference over the Truncated Gaussian by $\ln \mathcal{B} = 1 \sim 1.5$.

The inferred population parameters for NS and BH mass distribution models are presented in Table 3. The results for NS mass distribution are inferred by the Double Gaussian, Single Gaussian, and Uniform models, assuming a BH mass

¹ We take the ‘‘O3actual’’ PSD, which is available at <https://dcc.ligo.org/LIGO-T2000012/public>, for the events except GW170817. Since GW170817 was detected in O2, the noise curve can be approximated by the Early High Sensitivity curve in Abbott et al. (2018)

Table 2. Logarithm Bayes factors of the NS and BH mass distribution models.

$\ln \mathcal{B}$	NS mass distribution models			
	Double Gaussian	Single Gaussian	Uniform	Galactic
BH mass distribution models				
Truncated Gaussian	0	-0.16	-0.30	1.49
Truncated Power Law	1.09	1.11	1.13	2.68

Note. The values are relative to the evidence of Double Gaussian (NS mass distribution model) + Truncated Gaussian (BH mass distribution model).

distribution model of Truncated Power Law, and the results for BH mass distribution are obtained using Truncated Power Law and Truncated Gaussian models, assuming a NS mass distribution model of Double Gaussian (Actually the results assuming other BH mass distribution model/ NS mass distribution models are rather similar). In order to be more intuitive, we plot the mass distributions of BHs/NSs as shown in Fig. 1. For the Double Gaussian model of NS mass distribution, it is clear that there is a peak around $1.35M_{\odot}$, which is consistent with the first peak found in the mass distribution of Galactic NSs, but there is no peak in the higher mass range (around $1.9M_{\odot}$, for example). As for the Single Gaussian model, there is no significant peak. In comparison to the Uniform model, there is a moderate bulge in the low mass range (i.e., $1.2M_{\odot} \sim 1.6M_{\odot}$). The low mass cutoff of the BHs is constrained to $5.56^{+0.89}_{-1.34}M_{\odot}$ ($4.57^{+1.26}_{-1.33}M_{\odot}$) by the Truncated Power Law (Truncated Gaussian) model, however the high mass cutoff of BHs in NSBHs is constrained rather poor by either model. The spectrum index of Truncated Power Law is $6.21^{+4.47}_{-4.17}$, which seems larger than that of BHs in BBH populations (Abbott et al. 2021c). A steep spectrum index indicates that the BH mass distribution maybe narrow and may also be represented with a Gaussian (Özel et al. 2010). Interestingly, the mass distribution of BHs obtained by the Truncated Gaussian, i.e., $\mu_{\text{BH}} = 6.81^{+2.77}_{-1.46}M_{\odot}$ and $\sigma_{\text{BH}} = 2.74^{+4.84}_{-1.62}M_{\odot}$ is consistent with that constrained by the observations of X-ray binaries in the Galaxy (Özel et al. 2010). The fraction of BNS mergers in the NSBH and BNS population is $0.67^{+0.20}_{-0.31}$ (assuming Truncated Power Law + Double Gaussian model), and it is rather similar in all the synthesis models. This estimated fraction r_{BNS} is consistent with the merger rate densities of BNS (i.e., $320^{+490}_{-240}\text{Gpc}^{-3}\text{yr}^{-1}$ obtained by Abbott et al. (2021b)) and NSBH (i.e., $130^{+142}_{-69}\text{Gpc}^{-3}\text{yr}^{-1}$ obtained by Abbott et al. (2021a); see also Li et al. (2017) for a NSBH merger rate $\geq 100\text{Gpc}^{-3}\text{yr}^{-1}$ based on the kilonova modeling).

As for the spin properties of the binaries, the posterior distribution obtained by the Truncated Power Law + the Double Gaussian model is shown in Fig. 2, and the results from other models are similar. Though the distribution of misalignment is not well constrained, it is quite clear that a perfectly aligned spin distribution ($\sigma_t = 0$, $\zeta = 1$) has been ruled out (see also Abbott et al. (2021c) for the same conclusion for BBHs), while a purely isotropic distribution of spin orientation ($\sigma_t > 2$) is still allowed by the current data. The distribution of BHs' dimensionless spin magnitudes is constrained to $\mu_{\text{a}}^{\text{BH}} = 0.11^{+0.17}_{-0.10}$ and $\sigma_{\text{a}}^{\text{BH}} = 0.10^{+0.12}_{-0.09}$, but the distribution for NSs is just poorly constrained. We do not expect to determine the population properties of spins of these kinds of binaries with currently limited observations, while the correlation between the spin parameters and the component masses of the compact binaries will influence the inference of mass distribution of NSs that observed in GW signals (Ng et al. 2018), so it is helpful to incorporate the spin information into our population inference.

4. CONCLUSION AND DISCUSSION

We perform hierarchical population inferences for the GW binaries involving at least one NS, and construct several synthesis models that include both the component masses and spin properties of the BNS and NSBH binaries, since there is a correlation between the component masses and the spin properties of compact binaries (Pratten et al. 2020; Abbott et al. 2021a). We have also performed inferences without spin information for comparison, and find that the corresponding evidence is slightly smaller than the inferences with spin information, e.g., $\ln \mathcal{B} = \ln E_{\text{with spin}} - \ln E_{\text{no spin}} = 0.5$ for Double Gaussian NS mass distribution model + Truncated Power Law BH mass distribution model². The results are similar to those reported in Table 2, while for the peak of Double Gaussian model, the one in the spin-uninformative case is not as significant as the one in the spin-informative case. So it is helpful to take the

² For the case without spin information, we define the spin model as the default prior $\pi_{\phi}(\theta)$ that used for single event parameter estimation.

Table 3. Inferred population parameters of the NS and BH mass distribution models.

Parameters	NS mass distribution models assuming Truncated Power Law BH mass distribution model		
	Double Gaussian	Single Gaussian	Uniform
$m_{\min}[M_{\odot}]$	$1.11^{+0.15}_{-0.17}$	$1.12^{+0.14}_{-0.17}$	$1.15^{+0.12}_{-0.19}$
$m_{\max}[M_{\odot}]$	$2.12^{+0.68}_{-0.26}$	$1.99^{+0.54}_{-0.16}$	$1.96^{+0.26}_{-0.12}$
$\mu_1(\mu)[M_{\odot}]$	$1.33^{+0.26}_{-0.22}$	$1.41^{+0.35}_{-0.26}$	-
$\mu_2[M_{\odot}]$	$1.63^{+0.38}_{-0.31}$	-	-
$\sigma_1(\sigma)[M_{\odot}]$	$0.41^{+0.49}_{-0.34}$	$0.53^{+0.40}_{-0.29}$	-
$\sigma_2[M_{\odot}]$	$0.52^{+0.41}_{-0.40}$	-	-
r_1	$0.57^{+0.37}_{-0.47}$	-	-
r_{BNS}	$0.67^{+0.20}_{-0.31}$	$0.67^{+0.20}_{-0.29}$	$0.68^{+0.20}_{-0.30}$
BH mass distribution models assuming NS mass distribution model of Double Gaussian			
	Truncated Power Law	Truncated Gaussian	
$m_{\text{low}}[M_{\odot}]$	$5.56^{+0.89}_{-1.34}$	$4.57^{+1.26}_{-1.33}$	
$m_{\text{up}}[M_{\odot}]$	$18.83^{+9.54}_{-7.89}$	$19.02^{+9.32}_{-8.18}$	
α	$6.21^{+4.47}_{-4.17}$	-	
$\mu_{\text{BH}}[M_{\odot}]$	-	$6.81^{+2.77}_{-1.46}$	
$\sigma_{\text{BH}}[M_{\odot}]$	-	$2.74^{+4.84}_{-1.62}$	

Note. The values represent the medians and symmetric 90% credible intervals of the parameters.

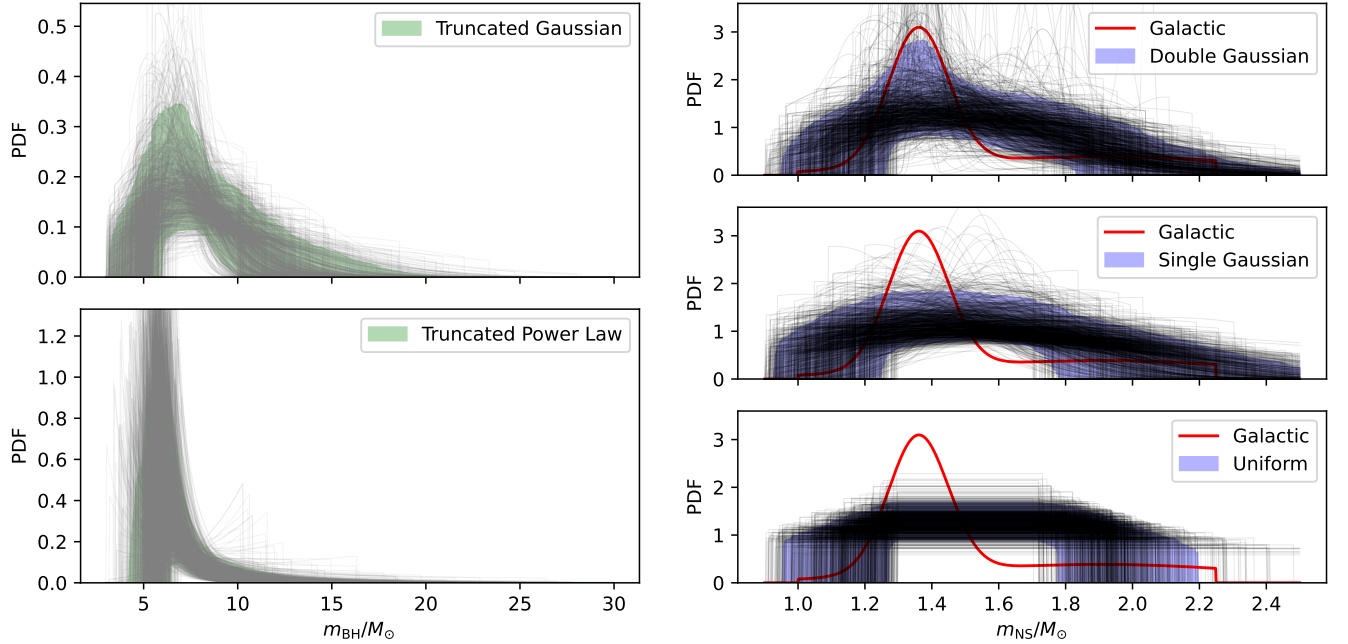


Figure 1. Mass distributions of NSs and BHs. The left column are the BH mass distributions obtained by Truncated Gaussian and Truncated Power Law, assuming the NS mass distribution model of Double Gaussian. The right column are the NS mass distributions obtained by Double Gaussian, Single Gaussian, and Uniform models, respectively, and their partner model for BH mass is the Truncated Power Law. The red curve represents the mass distribution of the Galactic NSs (i.e., the Double Gaussian model with $m_{\min} = 1M_{\odot}$, $m_{\max} = 2.25M_{\odot}$, $\mu_1 = 1.36M_{\odot}$, $\sigma_1 = 0.09M_{\odot}$, $\mu_2 = 1.9M_{\odot}$, $\sigma_2 = 0.5M_{\odot}$, and $r = 0.65$, as reported in Shao et al. (2020)). In each panel, the shaded region represents the 90% credible interval, and the grey lines are the 1000 independent posterior samples.

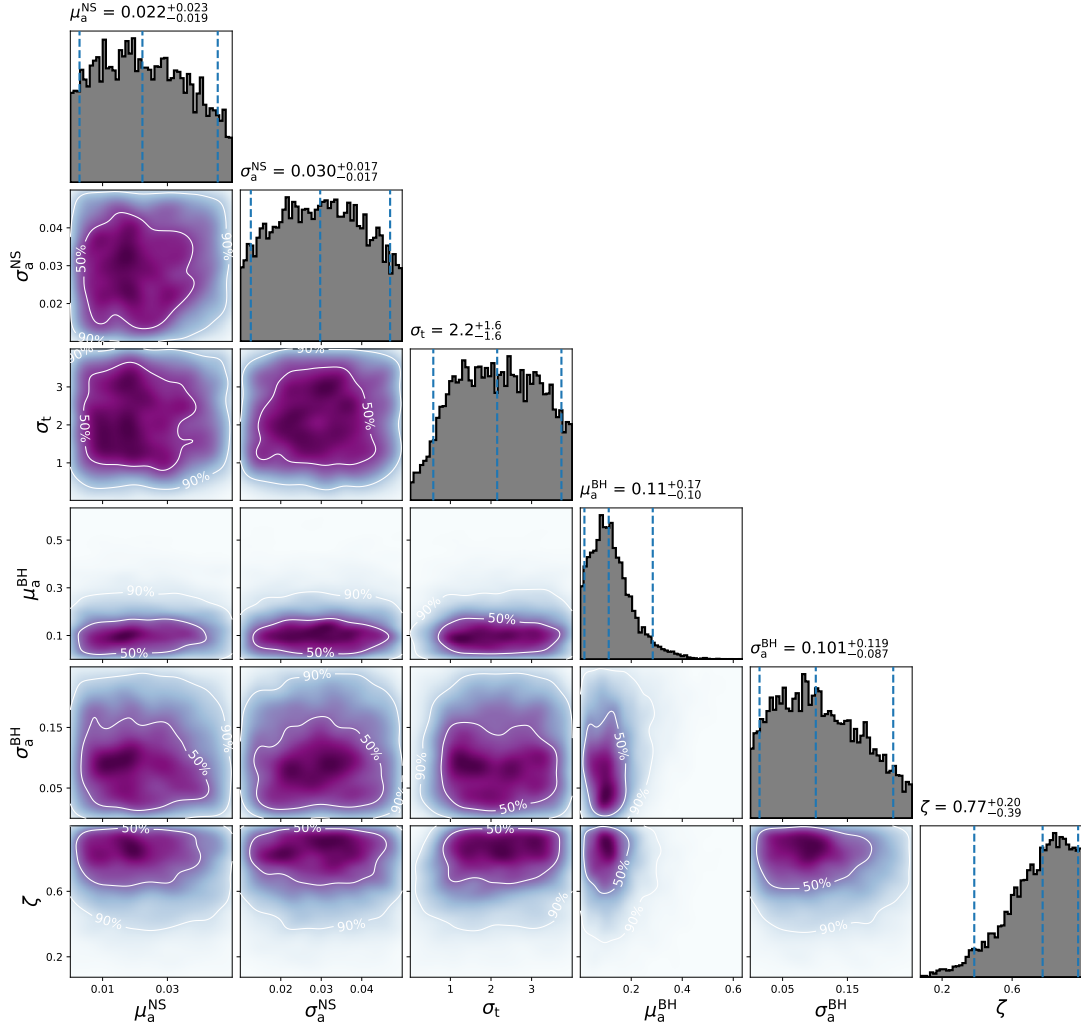


Figure 2. Posterior distribution for the spin model described in Sec. 2.2, assuming the Truncated Power Law BH mass function model and Double Gaussian NS mass distribution model. The contours represent 50% and 90% credible bounds, respectively.

spin information into consideration when inferring the mass distribution of the compact binaries, though we do not aim to determine the spin properties of these kinds of binaries by currently limited observations.

Our main conclusion is that the three NS mass distribution models (i.e., Double Gaussian, Single Gaussian, and Uniform) can not be reliably distinguished by current data. Our result is similar to Landry & Read (2021), where it is found that the Flat (in this work we call the Uniform) and Bimodal (i.e., the Double Gaussian in this work) models are equally preferred using the Akaike information criterion (Akaike 1981). Nevertheless, there is a significant peak in the mass distribution obtained in our Double Gaussian model, and the location of the peak resembles that of Galactic NSs (Shao et al. 2020). We further find that the mass distribution of Galactic NSs (Shao et al. 2020) is slightly more preferred than the other models (by $\ln \mathcal{B} \sim 1.5$), which indicates that the NSs observed via GW signals may have the similar mass distribution as the NSs identified by electromagnetic observation in the Galaxy. This conclusion is different from Landry & Read (2021), where the authors find that the mass distribution of the NSs observed via GWs is unimodal, predicting far fewer low-mass and moderately more high-mass NSs in the population. This difference may be

caused by the inclusion of the spin information of compact binaries into our hierarchical population inference. Another reason is that Landry & Read (2021) use a uniform distribution for BH masses with a pairing function $p(q) \propto q^{\beta_q}$ for NSBHs, while we use the more appropriate models for BH masses as indicated by Özel et al. (2010).

Both the BH mass distribution models indicate a narrow distribution located in $5 \sim 10M_{\odot}$, which is consistent with the BHs in the Galactic X-ray binaries (Özel et al. 2010). As for the population of the compact binaries involving at least one NS, a fraction of $\sim 70\%$ is BNSs, and this result agrees with the merger rate densities of BNS and NSBH estimated by Abbott et al. (2021b) and Abbott et al. (2021a). Due to the currently limited sample and the measurement uncertainties of NS spins, the distribution of NS spin magnitudes is not well constrained. From the inferred result of spin orientations, we conclude that a perfectly aligned spin distribution can be ruled out, but a purely isotropic distribution of spin orientation is still allowed by the GW data.

Encouragingly, LVKC will start their O4 and O5 observing runs in the next few years, at that time the sensitivities of GW detectors will be significantly improved (Abbott et al. 2018), and detection number of such binaries like NSBHs and BNSs will grow up quickly. Then the details of the mass distribution for NSs in compact binary mergers will be revealed, and the formation/evolution processes for BNS and NSBH systems will also be better understood.

ACKNOWLEDGMENTS

This work was supported in part by NSFC under grants of No. 11921003, No. 11703098, and and 12073080, the Chinese Academy of Sciences via the Strategic Priority Research Program (Grant No. XDB23040000), Key Research Program of Frontier Sciences (No. QYZDJ-SSW-SYS024). This research has made use of data and software obtained from the Gravitational Wave Open Science Center (<https://www.gw-openscience.org>), a service of LIGO Laboratory, the LIGO Scientific Collaboration and the Virgo Collaboration. LIGO is funded by the U.S. National Science Foundation. Virgo is funded by the French Centre National de Recherche Scientifique (CNRS), the Italian Istituto Nazionale della Fisica Nucleare (INFN) and the Dutch Nikhef, with contributions by Polish and Hungarian institutes.

Software: Bilby (Ashton et al. 2019, version 0.5.5, ascl:1901.011, <https://git.ligo.org/lscsoft/bilby/>), Dynesty (Speagle 2020), PyCBC (Biwer et al. 2019; Nitz et al. 2019, gwastro/pycbc: PyCBC Release v1.14.1, <https://github.com/gwastro/pycbc/tree/v1.14.1>)

REFERENCES

- Abbott, B. P., Abbott, R., Abbott, T. D., et al. 2016, PhRvL, 116, 061102, doi: [10.1103/PhysRevLett.116.061102](https://doi.org/10.1103/PhysRevLett.116.061102)
- . 2017, PhRvL, 119, 161101, doi: [10.1103/PhysRevLett.119.161101](https://doi.org/10.1103/PhysRevLett.119.161101)
- . 2018, Living Reviews in Relativity, 21, 3, doi: [10.1007/s41114-018-0012-9](https://doi.org/10.1007/s41114-018-0012-9)
- . 2019, Physical Review X, 9, 031040, doi: [10.1103/PhysRevX.9.031040](https://doi.org/10.1103/PhysRevX.9.031040)
- . 2020a, ApJL, 892, L3, doi: [10.3847/2041-8213/ab75f5](https://doi.org/10.3847/2041-8213/ab75f5)
- Abbott, R., Abbott, T. D., Abraham, S., et al. 2020b, ApJL, 896, L44, doi: [10.3847/2041-8213/ab960f](https://doi.org/10.3847/2041-8213/ab960f)
- . 2020c, PhRvL, 125, 101102, doi: [10.1103/PhysRevLett.125.101102](https://doi.org/10.1103/PhysRevLett.125.101102)
- . 2021a, ApJL, 915, L5, doi: [10.3847/2041-8213/ac082e](https://doi.org/10.3847/2041-8213/ac082e)
- . 2021b, Physical Review X, 11, 021053, doi: [10.1103/PhysRevX.11.021053](https://doi.org/10.1103/PhysRevX.11.021053)
- . 2021c, ApJL, 913, L7, doi: [10.3847/2041-8213/abe949](https://doi.org/10.3847/2041-8213/abe949)
- Akaike, H. 1981, Journal of Econometrics, 16, 3, doi: [https://doi.org/10.1016/0304-4076\(81\)90071-3](https://doi.org/10.1016/0304-4076(81)90071-3)
- Alsing, J., Silva, H. O., & Berti, E. 2018, MNRAS, 478, 1377, doi: [10.1093/mnras/sty1065](https://doi.org/10.1093/mnras/sty1065)
- Ashton, G., Hübner, M., Lasky, P. D., et al. 2019, Bilby: Bayesian inference library. <http://ascl.net/1901.011>
- Biwer, C. M., Capano, C. D., De, S., et al. 2019, PASP, 131, 024503, doi: [10.1088/1538-3873/aaef0b](https://doi.org/10.1088/1538-3873/aaef0b)
- Han, M.-Z., Tang, S.-P., Hu, Y.-M., et al. 2020, ApJL, 891, L5, doi: [10.3847/2041-8213/ab745a](https://doi.org/10.3847/2041-8213/ab745a)
- Jin, Z.-P., Li, X., Cano, Z., et al. 2015, ApJL, 811, L22, doi: [10.1088/2041-8205/811/2/L22](https://doi.org/10.1088/2041-8205/811/2/L22)
- Kalogera, V. 2000, ApJ, 541, 319, doi: [10.1086/309400](https://doi.org/10.1086/309400)
- Landry, P., & Read, J. S. 2021, arXiv e-prints, arXiv:2107.04559. <https://arxiv.org/abs/2107.04559>
- Li, X., Hu, Y.-M., Jin, Z.-P., Fan, Y.-Z., & Wei, D.-M. 2017, ApJL, 844, L22, doi: [10.3847/2041-8213/aa7fb2](https://doi.org/10.3847/2041-8213/aa7fb2)

- Li, Y.-J., Han, M.-Z., Tang, S.-P., et al. 2020, arXiv e-prints, arXiv:2012.04978.
<https://arxiv.org/abs/2012.04978>
- Li, Y.-J., Wang, Y.-Z., Han, M.-Z., et al. 2021, *The Astrophysical Journal*, 917, 33,
doi: [10.3847/1538-4357/ac0971](https://doi.org/10.3847/1538-4357/ac0971)
- Ng, K. K. Y., Vitale, S., Zimmerman, A., et al. 2018, *PhRvD*, 98, 083007, doi: [10.1103/PhysRevD.98.083007](https://doi.org/10.1103/PhysRevD.98.083007)
- Nitz, A., Harry, I., Brown, D., et al. 2019, *gwastro/pycbc: PyCBC Release v1.14.4, v1.14.4*, Zenodo,
doi: [10.5281/zenodo.3546372](https://doi.org/10.5281/zenodo.3546372)
- Özel, F., & Freire, P. 2016, *ARA&A*, 54, 401,
doi: [10.1146/annurev-astro-081915-023322](https://doi.org/10.1146/annurev-astro-081915-023322)
- Özel, F., Psaltis, D., Narayan, R., & McClintock, J. E. 2010, *ApJ*, 725, 1918,
doi: [10.1088/0004-637X/725/2/1918](https://doi.org/10.1088/0004-637X/725/2/1918)
- Pratten, G., Schmidt, P., Buscicchio, R., & Thomas, L. M. 2020, *Physical Review Research*, 2, 043096,
doi: [10.1103/PhysRevResearch.2.043096](https://doi.org/10.1103/PhysRevResearch.2.043096)
- Qin, Y., Fragos, T., Meynet, G., et al. 2018, *A&A*, 616, A28, doi: [10.1051/0004-6361/201832839](https://doi.org/10.1051/0004-6361/201832839)
- Qin, Y., Marchant, P., Fragos, T., Meynet, G., & Kalogera, V. 2019, *ApJL*, 870, L18, doi: [10.3847/2041-8213/aaf97b](https://doi.org/10.3847/2041-8213/aaf97b)
- Rodriguez, C. L., Zevin, M., Pankow, C., Kalogera, V., & Rasio, F. A. 2016, *ApJL*, 832, L2,
doi: [10.3847/2041-8205/832/1/L2](https://doi.org/10.3847/2041-8205/832/1/L2)
- Safarzadeh, M., & Wysocki, D. 2021, *ApJL*, 907, L24,
doi: [10.3847/2041-8213/abd8c7](https://doi.org/10.3847/2041-8213/abd8c7)
- Shao, D.-S., Tang, S.-P., Jiang, J.-L., & Fan, Y.-Z. 2020, *PhRvD*, 102, 063006, doi: [10.1103/PhysRevD.102.063006](https://doi.org/10.1103/PhysRevD.102.063006)
- Speagle, J. S. 2020, *MNRAS*, 493, 3132,
doi: [10.1093/mnras/staa278](https://doi.org/10.1093/mnras/staa278)
- Stovall, K., Freire, P. C. C., Chatterjee, S., et al. 2018, *ApJL*, 854, L22, doi: [10.3847/2041-8213/aaad06](https://doi.org/10.3847/2041-8213/aaad06)
- Tang, S.-P., Li, Y.-J., Wang, Y.-Z., Fan, Y.-Z., & Wei, D.-M. 2021, arXiv e-prints, arXiv:2107.08811.
<https://arxiv.org/abs/2107.08811>
- Tang, S.-P., Wang, H., Wang, Y.-Z., et al. 2020, *ApJ*, 892, 56, doi: [10.3847/1538-4357/ab77bf](https://doi.org/10.3847/1538-4357/ab77bf)
- Thrane, E., & Talbot, C. 2019, *PASA*, 36, e010,
doi: [10.1017/pasa.2019.2](https://doi.org/10.1017/pasa.2019.2)
- Tiwari, V. 2018, *Classical and Quantum Gravity*, 35, 145009, doi: [10.1088/1361-6382/aac89d](https://doi.org/10.1088/1361-6382/aac89d)
- Vitale, S., Lynch, R., Sturani, R., & Graff, P. 2017, *Classical and Quantum Gravity*, 34, 03LT01,
doi: [10.1088/1361-6382/aa552e](https://doi.org/10.1088/1361-6382/aa552e)
- Wang, Y.-Z., Tang, S.-P., Liang, Y.-F., et al. 2021, *ApJ*, 913, 42, doi: [10.3847/1538-4357/abf5df](https://doi.org/10.3847/1538-4357/abf5df)
- Yang, B., Jin, Z.-P., Li, X., et al. 2015, *Nature Communications*, 6, 7323, doi: [10.1038/ncomms8323](https://doi.org/10.1038/ncomms8323)
- Zhu, X., Thrane, E., Osłowski, S., Levin, Y., & Lasky, P. D. 2018, *PhRvD*, 98, 043002,
doi: [10.1103/PhysRevD.98.043002](https://doi.org/10.1103/PhysRevD.98.043002)